Experimental investigation on adhesively bonded U-shaped metallic joints using the Arcan test

R. Ciardiello [a,*], L. Greco [a], M. Miranda [a], F. Di Sciullo [b], L. Goglio [a]

[a] Department of Mechanical and Aerospace Engineering, Politecnico di Torino, Corso Duca degli Abruzzi 24, Turin 10129, Italy
[b] Fiat Research Center, Corso Luigi Settembrini, 40, 10135 Turin, Italy

ABSTRACT

An experimental investigation on adhesively bonded joints has been carried out by using an adhesive used in automotive applications. The main goal of this work is to characterize the mechanical behaviour of the adhesive joints subjected to different loading angles and understand whether the cataphoresis painting process can be used to cure the adhesive. To this aim, two different typical temperatures, used for the cataphoresis process, have been used for curing the studied adhesive. Arcan test has been used to characterize the mechanical behaviour of the adhesive joints by using five different loading angles: 0° (shear condition), 30°, 45°, 60° (combined shear-tensile), and 90° (tensile). The experimental tests showed that the adopted curing cycles conducted at 190 °C for 15′ and 160 °C for 45′ are both able to fully cure the adhesive, this was verified with Differential Scanning Calorimeter analysis (DSC). The two curing temperatures do not lead to significant differences in the maximum values of the strength. Arcan test conducted at different loading angles shows that the maximum value of the strength is obtained for the condition of shear loading (about 10 MPa nominal strength), while the lowest value is related to the condition of tensile loading (about 5 MPa nominal strength). Scanning Electron Microscope (SEM) analysis was used to assess the distribution of the hollow glass spheres that are embedded in this adhesive to set the thickness layer.

Introduction

The use of the adhesives has progressively increased, and it is constantly growing, over the last few decades in many industrial areas such as automotive, marine, and aerospace industries (Banea and da Silva, 2009; Rudawska, 2010; Casalegno et al., 2018). In automotive industry especially, the market requires lighter vehicles to reduce fuel consumption and CO_2 emissions (Ciardiello et al., 2019). This goal is pursued by using lighter components and materials, especially structural parts, such as metal alloys or composite materials (Jambor and Beyer, 1997; Li et al., 2004). In this scenario, adhesive bonding represents a major asset and a very good alternative to traditional mechanical assembly techniques as bolting and welding. Adhesive bonding offers a more uniform distribution of stress, can join small components, can prevent or reduce the corrosion between dissimilar materials and does not require holes that can introduce cracks in the structures (Banea and da Silva, 2009; da Silva et al., 2011; Belingardi and Chiandussi, 2004). On the other hand, adhesive joints are affected by their service environments and they are difficult to disassemble for inspection and repair (Kim et al., 1997).

Epoxy-based adhesives are widely used in the automotive industry for their ability to bond a wide range of materials, even dissimilar, such as plastics, metals, rubbers and wood (Raftery et al., 2009). Epoxy adhesives are available in two-component (resin and hardener) products that can be cured also at room temperatures, but must be applied within a limited time span after mixing, and monocomponent adhesives that need elevated temperatures to be activated. For these reasons, monocomponent adhesives, in many cases, need to be cured in a relatively long time compared to the cycle time of the automotive assembly lines. This disadvantage encourages automotive industry to find an alternative way to cure these adhesives without lengthening the cycle time. The study that has been carried out in this work aims at assessing whether a monocomponent epoxy adhesive can be cured by using the temperatures involved in the cataphoresis process. Morano et al. (2019) have already discussed the possible integration of structural adhesives in car body manufacturing by merging different operations. In particular, the possibility to apply adhesive in the body in white stage without any surface treatment and to accomplish the final cure during the backing process.

* Corresponding author.
E-mail addresses: raffaele.ciardiello@polito.it (R. Ciardiello), lucrezia.greco@studenti.polito.it (L. Greco), mauro.miranda@polito.it (M. Miranda), fiorenza.disciullo@crf.it (F.D. Sciullo), luca.goglio@polito.it (L. Goglio).

Therefore, two different temperatures and time cycles that are consistent with those adopted in the cataphoresis were chosen to understand whether these can cure the adhesive joint prepared with a monocomponent epoxy adhesive. The idea is to unify two long operations that are the curing procedure of a structural adhesive and the cataphoresis. In this work, a preliminary analysis has been carried out to verify if the typical temperatures and times used by cataphoresis can cure a monocomponent adhesive.

Another issue related to adhesive joints used in the automotive industry is that the most part of automotive components can be subjected to different loading directions during their life (Machado et al., 2017; Pirondi and Nicoletto, 2004). For this reason, it is very important to study the mechanical behaviour of adhesive joints subjected to different loading angles. Unfortunately, there is no standard test on adhesive that is able to characterise the adhesive to different loading angles. Standard tests are able to evaluate the mode I behaviour by using the Double Cantilever Beam (DCB) and the Tapered Double Cantilever Beam (TDCB) (ASTM D3433-99 2012; ISO 25217:2009 2009; BS 7991:2001 2001). On the other hand, there are no standard tests that univocally can study the mixed-mode I/II and mode alone II for adhesives (Stamoulis et al., 2016). Tests such as Mixed Mode Bending (ASTM D6671/D6671M-19 2013), End Notched Flexure (ASTM D7905/7905 M 2014) and Calibrated End-Loaded Split (ISO/DIS 15114:2014 2014) are used for this purpose. Furthermore, Stamoulis et al. (2016) report several non standard tests that are used for the assessment of adhesive joints under mixed mode conditions. Of course, the execution of these tests can be time consuming and involves different kinds of specimens and different equipment. Amongst the traditional tests, the Arcan fixture can be used to load a material or a bonded structure at different angles, also considering mixed-mode I/II, by simply varying the loading angle from 0° (tensile load) to 90° (shear) (Stamoulis et al., 2016; Argoud et al., 2018). The Arcan fixture (Arcan et al., 1987) allows for an easy assessment of the mechanical properties of the adhesive joints under different loading angles by simply rotating the fixture in the testing machine, without changing the specimen configuration. Furthermore, Legendre et al. (2018) found that the Arcan fixture is suitable to determine the properties of the interfaces in bonded joints by using energy and strain criteria.

In this work, double-U shaped (also called KS2 specimen) (Yang et al., 2010; Hörhold et al., 2016; Patil and Lankarani, 2019) specimens made of boron steel were prepared by using a monocomponent epoxy adhesive used in automotive industry. Mechanical tests were performed under five different loading angles by means of an Arcan fixture: 0° (tensile load), 30°, 45°, 60° (combined shear-tensile load), and 90° (shear load).The boron steel substrates were neither cleaned nor pre-treated, taking advantage of the capability reported by the technical datasheet which claims that this adhesive can bond also in presence of oils and lubricants. This characteristic makes this adhesive particularly attractive for automotive applications. Two different curing cycles were analysed, 15′ at 190 °C and 45′ at 160 °C . Temperatures in this range have been analysed also by García et al. (2007) that investigated the cure temperature effects on cataphoretic automotive primers. These curing cycles have been analysed since they are respectively the extreme conditions (respectively shorter time and higher temperature, longer time and lower temperature) of the cataphoresis cycles. DSC analysis was used to verify whether the adhesive is fully cured and SEM analysis was used to assess the dispersion of the hollow glass spheres included in the adhesive matrix.

Materials and methods

The substrates used in this work are made of a boron alloyed steel 21MnB5 (C 0.23%, Si 0.4, Mn 1.3% and B 0.005%). Table 1 presents the mechanical properties of this material. Fig. 1a) shows the main size of the U-shaped specimens. The substrates have a thickness of 1.2 mm and are galvanized.

Table 1
Mechanical properties of the substrates.

Yield strength [MPa]	700
Tensile strength [MPa]	950
Elastic modulus [GPa]	200
Elongation at break [%]	14

Table 2
Mechanical properties of the adhesive.

Tensile strength [MPa]	35
Elastic modulus [MPa]	2000
Elongation at break [%]	5

This type of specimen, typical of car body manufacturing (Argoud et al., 2018), was originally conceived to test the strength of a spot welds (Yang et al., 2010; Hörhold et al., 2016; Patil and Lankarani, 2019), executed in the centre of the rectangular zone of overlap (90 mm x 22 mm). Within this work, it was adapted by adhesively bonding a central zone, as bonding the whole overlap, would create a joint much stronger than the substrates that would be fail first during the test. To do so, polyester foils were inserted to delimit the bonded area (and at the same time define the desired adhesive thickness, as shown in Fig. 1).

The adhesive used in this study is Betaforce 1640 G, a one-component epoxy supplied by Dow Automotive. The mechanical properties of the Betaforce 1640 G are reported Table 2. These values were obtained by testing dogbone specimens. Betaforce 1640 G presents a glass transition temperature of 108 °C (this value was brovided by the datasheet).

This adhesive was modified by the manufacturer with some fillers, hollow glass spheres and some minerals. The supplier does not give information on the filling materials. SEM analysis and Thermo-Gravimetric Analysis (TGA), Sections 3.2 and 3.3, showed the presence of hollow glass spheres and a final weight concentration after the TGA of 35%. SEM analysis, in Section 3.3, showed that the hollow glass spheres have an average size of 70 μm with a wide scatter (±20 μm). In general, glass spheres are used to easily obtain the adhesive thickness of the adhesive joints. However, the size and the scatter of the particles do not allow for reaching the typical adhesive thickness usual for epoxy adhesives, that is about 0.2 mm. For this reason, the following bonding procedure was adopted.

As previously said, no superficial pre-treatment was carried out on the boron steel surfaces as adhesion promoter and the substrates were bonded as received from the bending press process. The adhesive thickness of the joint was obtained by using two polyester foils (thickness of 0.2 mm) that were used to define the bonding length, which is 30 mm, as shown in Fig. 1b). Polyester foils were chosen since they do not interact with adhesive and substrates. The bonding pressure was assured by an equipment that is able to lead the two substrates at the desired thickness and that can keep the pressure also during the curing process, as shown in Fig. 1c). The bonding procedure was validated as preliminary analysis by bonding five different specimens and by cutting the specimens in the middle (in the longitudinal direction) to directly measure the adhesive thickness, as shown in Fig. 1c). This procedure was validated since it led to a scatter lower than 0.03 mm for all the analysed cases. Two different curing cycles were adopted: 15′ at 190 °C and 45′ at 160 °C.

The Arcan fixture used in this work is shown in Fig. 2 together with the testing conditions considered in this work. The adopted configurations are: 0°, 30°, 45°, 60° and 90°. The tests were performed with a Galdabini testing machine, equipped with a 100 kN loadcell, at a speed of 10 mm/min. Five replications were carried out for each configuration.

FE-SEM analysis was carried out with a Zeiss SUPRA40. An accelerating voltage of 10 kV was used together with secondary emission signal. The specimens were properly coated with a gold layer of 10 nm. The
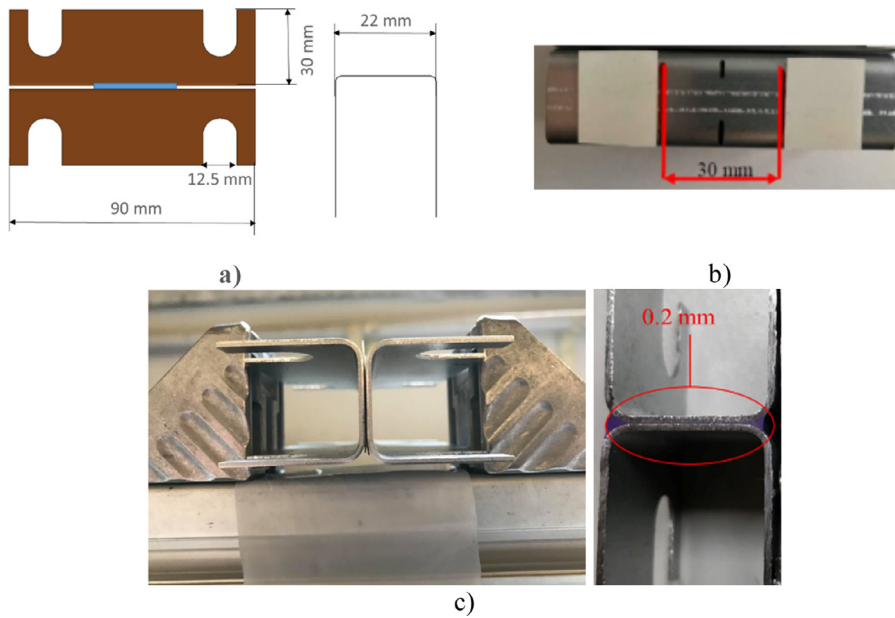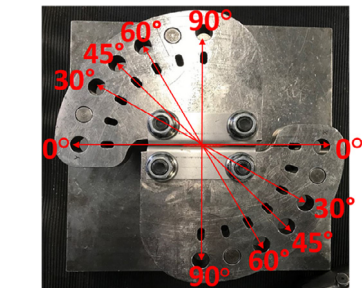
Fig. 2. Testing angles adopted in this work.

energy dispersive X-ray spectrometry (EDS) associated to SUPRA40 was used to assess the clearer elements visible in SEM analysis.

Thermo-Gravimetric Analysis (TGA) was carried out to assess the curing degree of the adhesive, using a TGA-SDT851 (Mettler Toledo) instrument under inert atmosphere (100 mL/min flow rate). Samples were preliminarly heated from 25 °C to 100 °C at a rate of 10 °C/min, held isothermally for 60 min to remove any residual moisture/solvents

before ramping to 800 °C. A DSC 1 STAR (Matter Toledo) instrument was used to collect DSC thermograms. The DSC measurements were performed with standard aluminium pans under nitrogen atmosphere (50 cm^3/min) and with a 10 °C/min heating rate, from 25 °C up to 200 °C.

Results

In this section, the Arcan tests, the TGA, the DSC and the SEM analyses are presented. The mechanical tests conducted on joints under different loading angles are indicated as 0° for the shear test; 30°, 45° and 60° indicate the tests conducted under combined load; 90° indicates the joints subjected to pure tensile load.

Arcan tests

Representative curves of the Arcan tests conducted on adhesive joints under the different loading angles are shown in Fig. 3. In particular, Fig. 3a) displays the load-displacement curves related to the specimens cured 45 min at 160 °C while Fig. 3b) shows representative curves, for the same loading angles, related to the specimens cured 15 min at 190 °C. The same scale is used to easily compare the two diagrams. Both
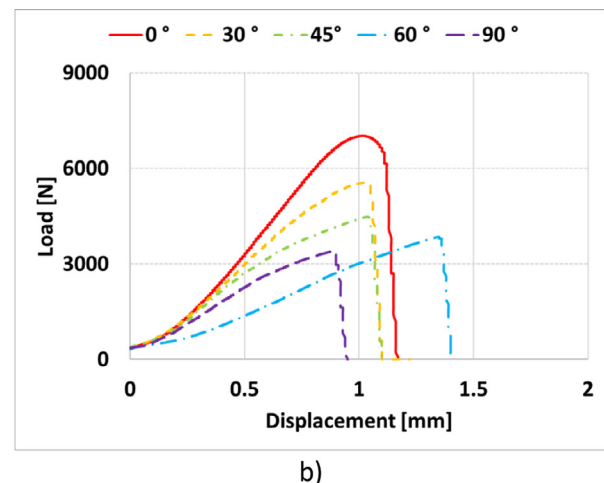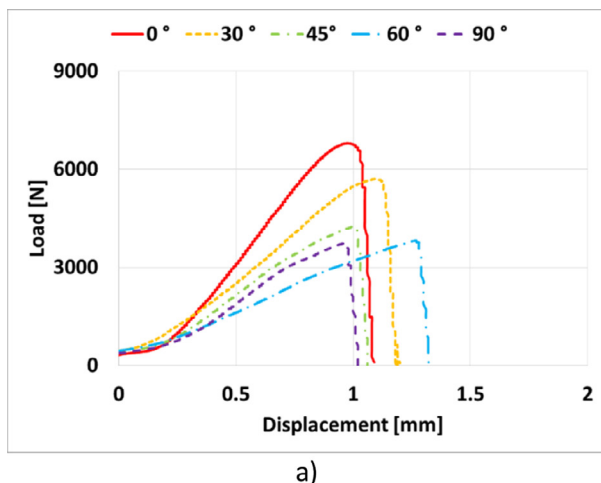

Fig. 3. load-displacement curves for the two different curing conditions: a) 45 min at 160 °C; b) 15 min at 190 °C.
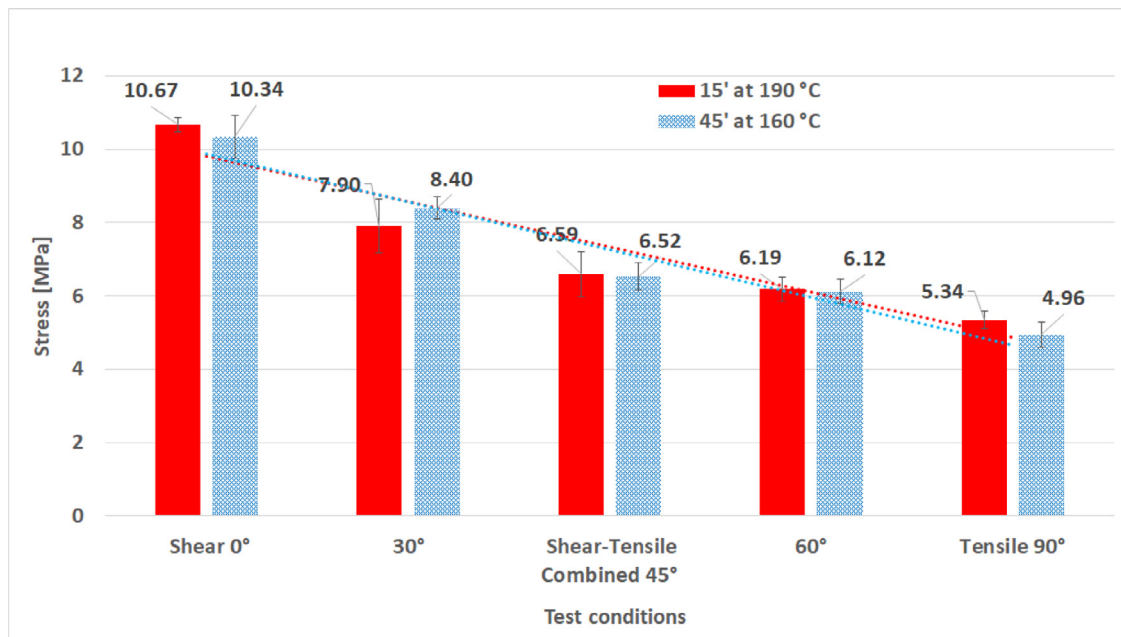
Fig. 4. Values of the stress for the different testing angles and the two different curing conditions.
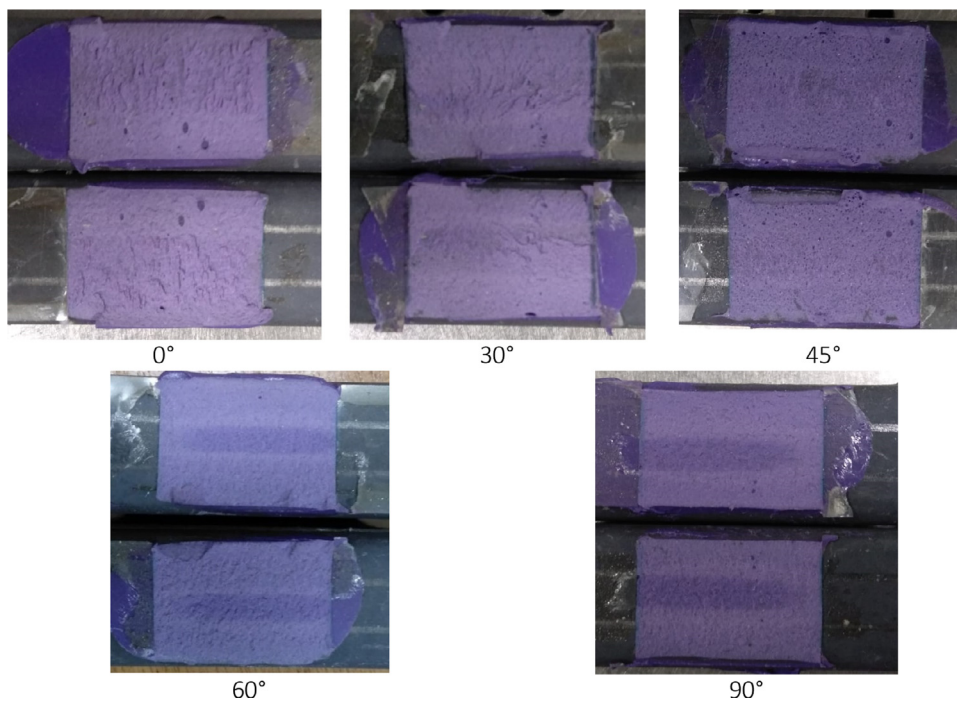

Fig. 5. Fracture surfaces for different testing angles.

show that the trends are quite similar for the two curing conditions. It is noticeable that the load rises softly up to a displacement of 0.3 mm in both diagrams. Then the increase is larger. This could be due to small clearances in the fixture. It is worth to note that the initial linear trends, after 0.3 mm, representative of the stiffness, decrease with the rise of the testing angle. The only exception is related to the specimen tested at 90° that presents a stiffness closer to the specimens that were tested with the angle of 45° and higher than 60°. This behaviour has been reported also in (Argoud et al., 2018). Furthermore, the curves related to the testing angle of 60° exhibits a slightly larger displacement compared to the other tested angles.

The maximum displacements are very close, between 1 mm and 1.4 mm, while the highest loads were found for the loading angle 0° in

both cases. The most significant drops of the maximum load, 20%, are between testing angles 0°–30° and 30°–45°. On the other hand, there is not a significant difference between the loading configuration 45° and 60° whereas there is a further decrease of 15% changing the loading configuration from 60° to 90°. This reduction can be attributed to the effect of the U-shape substrates that, in presence of the tensile stress, changes the mode of fracture exhibiting a path that starts from the sides and propagates towards the centre of the bonded area.

Fig. 4 shows the comparison of the maximum average stresses obtained for the various loading configurations and the two different curing conditions. The diagram shows that the load decreases with the increase of the testing angle for both conditions. The larger variations between the two different curing conditions are related to the testing
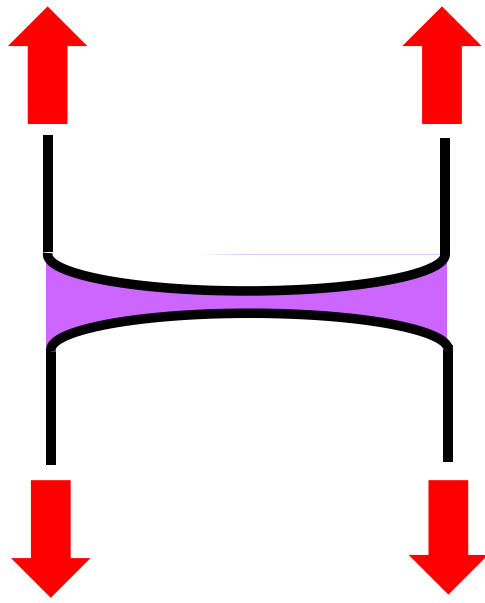
Fig. 6. Action of the loading from the lateral flanges to the central bonded zone in case of prevalent tensile loading.

Fig. 7. DSC analyses on the cured and uncured adhesive.

angles 30° and 90°. However, the standard deviations shown graphically by the error bars in the Figure do not allow to report a significant difference between the two values.

Fracture surfaces of the specimens are presented in Fig. 5. It is noticeable that the fractures were cohesive for the all considered cases. Only the fracture surfaces related to the curing condition at 190 °C for 15′ are reported here because they are similar for both the adopted curing condition. It is worth to note, that the fracture surfaces related to the testing angle 0° and 30° present some crests related to the prevalent shear loads involved in the test. On the other hand, the fracture surfaces from 45° to 90° present a fracture surface without crests. As written in the description of the mechanical properties, the reduction of the load can be related to the different responses of the adhesive to shear, compared to tensile condition. In particular, it is related to the U-shape of the substrates that, in the case of the tests where tensile loading is prevalent, change the mode of fracture from a general sliding mode to a peel-like mode that starts from the sides and propagates the cracks towards the centre of the bonded area. This occurs because the lateral flanges of the
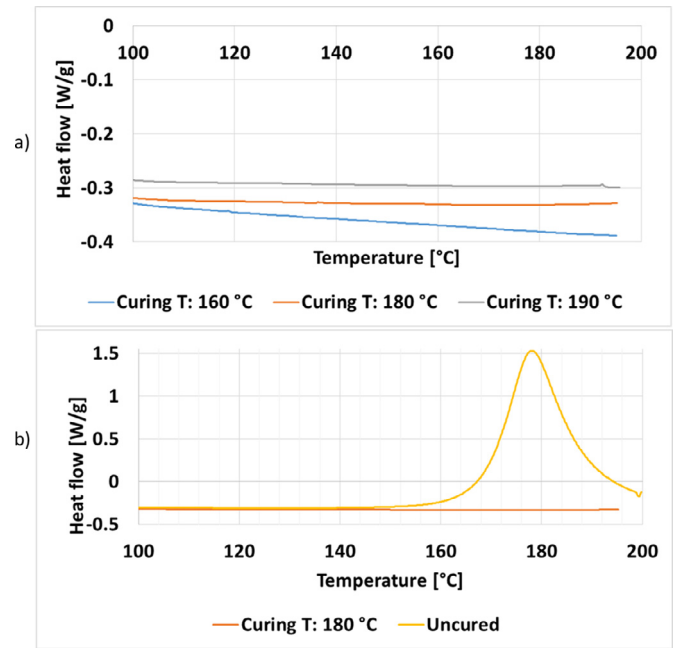
U specimen are the parts where the loads are applied and transmitted to the central bonded zone as sketched in Fig. 6. The effect is especially evident for the specimens fractured in the test conducted at 60° and 90°, where the central zone looks darker because it is the last that separated and thus it is not deformed plastically.

DSC and TGA analyses

DSC analyses were carried out in order to understand whether the adhesives were completely cured for the two adopted conditions. The heating process during the DSC analysis could induce an exothermic peak if the adhesive is not completely cured (Ooi et al., 2000). Fig. 7a) shows the DSC analyses of the three samples that were cured at three different temperatures: 45′ at 160 °C, 30′ at 180 °C (standard curing cycle recommended by the manufacturer) and 15′ at 190 °C. The diagram displays the curves in the temperature range of interest and shows the absence of exothermal or endothermal peaks. This means that the analysed samples are completely cured. Fig. 7b) shows the comparison
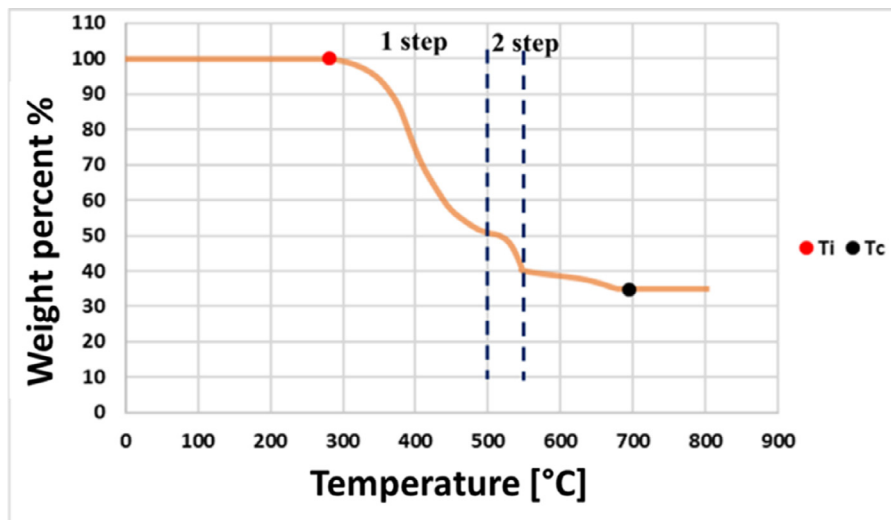
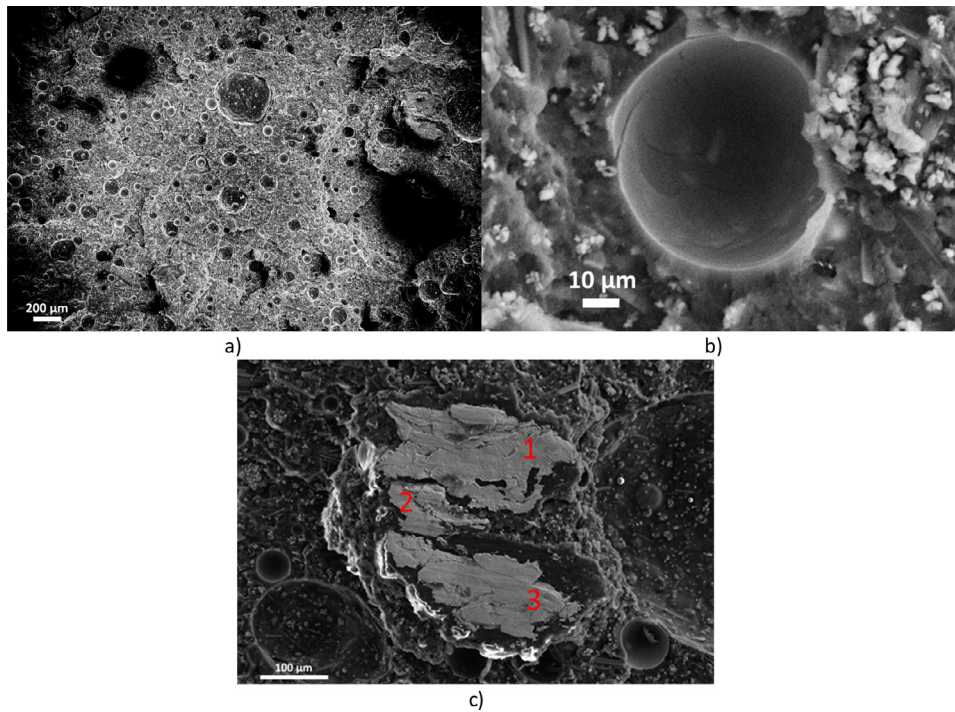**Fig. 8.** TGA analysis of the cured adhesive.

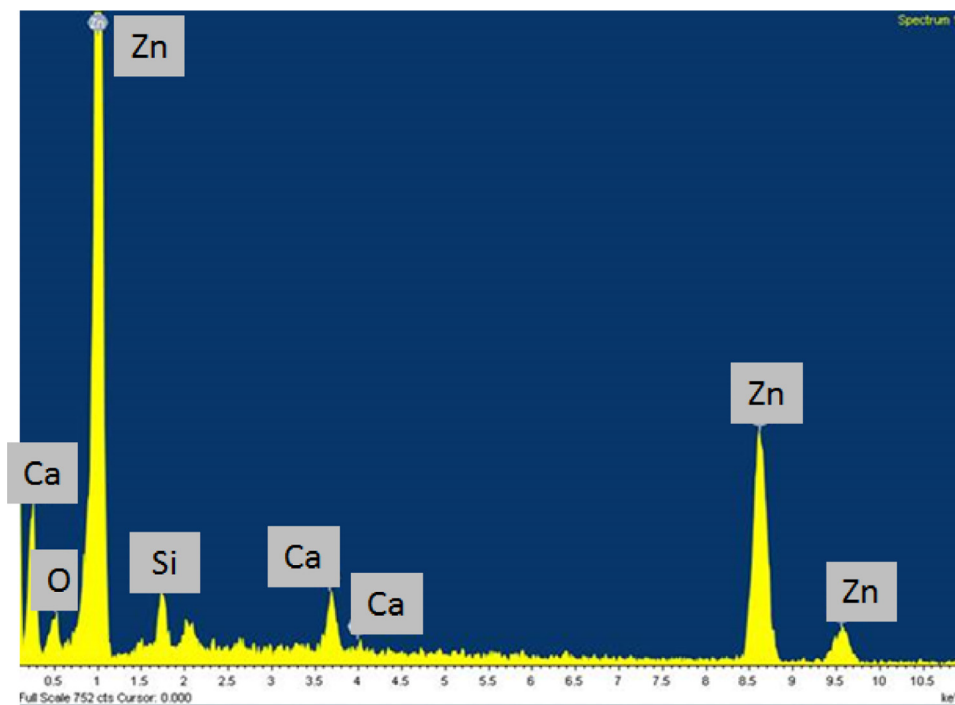**Fig. 9.** SEM analysis of the fractured joints.

Fig. 10. EDX spectrum of the clearer zone in Fig. 9c).

between the sample cured with the standard cycle and an uncured sample. In this case, the exothermic peak is considerably evident compared to the plateau exhibited by the cured sample. This analysis, together with the mechanical tests presented in the previous section, shows that the two adopted thermal cycles of the cataphoresis process are able to fully cure the adopted adhesive.

TGA analysis was performed to evaluate the percentage of the weight residual content that is not declared by the manufacturer. The thermogram in Fig. 7 shows that this weight content is 35%. The weight loss curve exhibits two significant weight drops, indicated in Fig. 8 as step 1 and 2 respectively. The initial degradation temperature T_i is 280 °C while the final one T_c is 695 °C.

SEM analysis

SEM analysis was carried out in order to show the distribution of the glass spheres that were found within the adhesive matrix and to verify the size of the hollow glass spheres since different works (Ciardiello et al., 2017) have shown that the nominal size of these spheres has a relatively large scatter. Fig. 9a) shows that the distribution of the particles is uniform and there is no presence of sphere agglomerates. Fig. 9b) shows a magnification of one sphere. The digital image correlation software of the SEM was able to measure an average value of the spheres which is 70 μm with a scatter of ±20 μm. Fig. 9c) displays a clearer material bonded on the matrix. The energy dispersive X-ray

analysis (EDX), associated with the SEM, showed that these are small parts of Zn exfoliated from the substrate. Fig. 9c) shows three different delaminated layers of the galvanic coating, indicated by the numbers in Fig. 9c). These layers were found on the fracture surfaces of all the five adopted configurations and for both the adopted curing conditions. Furthermore, SEM analysis clarified that these small delaminated layers were present throughout the surface and not in a limited area. Twenty different delaminated layers were measured by using SEM and digital image correlation technique. The average largest size of these particles was 180 μm with a scatter of 50 μm.

The spectrum of the EDX analysis of the clearer sample in Fig. 9c) is reported in Fig. 10. This analysis was able to assess the constituents detected on the sample. The analysed sample is mainly constituted by zinc with a percentage of 86%. Traces of calcium (Ca), oxygen (O) and silicon (Si) were found in the spectrum and can be connected to the presence of glass spheres in the adhesive (Si) and to the adhesive constituents (Ca, O). The traces of Zn are due to the galvanization process which this material undergoes.

Conclusions

The mechanical behaviour of adhesive joints prepared with a mono-component epoxy adhesive and U-shape boron steel substrates has been studied with regards to five different loading angles from pure tensile to shear tests. Two different curing conditions were tested in order to assess if the temperature of the cataphoresis process is suitable to cure the adhesive, so reducing the time cycle.

Mechanical tests showed that there is no significant difference between the adhesive cured in the two different conditions. The shear configuration (0°) led to the highest value of strength, with a reduction of 40% for the combined load (45°) and 50% for the tensile configuration (90°). This reduction can be related to the U-shape of the substrates that, in the case of the tensile test and the combinations shear-tensile, changes the mode of fracture with a crack path starting from the sides and propagating towards the centre of the bond. This is especially evident for the specimen fractured in the test conducted at 60° and 90° where the central zone that looks darker is the last that separated.

DSC analysis showed that both adopted curing conditions are able to completely cure the adhesive and TGA shows that the hollow glass spheres and the minerals are present in a percentage of 35%.

SEM analysis was used to display the presence of hollow glass spheres that are included in the adhesive matrix by the producer. The dispersion of these particles is uniform.

Declaration of Competing Interest

The authors declare that they have no known competing financial interests or personal relationships that could have appeared to influence the work reported in this paper.

References

Banea, M.D., da Silva, L.F.M., 2009. Adhesively bonded joints in composite materials: an overview. P. I. Mech. Eng. L.-J. Mat. 223, 1–18.

Rudawska, A., 2010. Adhesive joint strength of hybrid assemblies: Titanium sheet-composites and aluminium sheet-composites—Experimental and numerical verification. Int. J. Adhes. Adhes. 30 (7), 574–582.

Casalegno, V., Salvo, M., Rizzo, S., Goglio, L., Damiano, O., Ferraris, M., 2018. Joining of carbon fibre reinforced polymer to Al-Si alloy for space applications. Int. J. Adhes. Adhes. 82, 146–152.

Ciardiello, R., Belingardi, G., Martorana, B., Brunella, V., 2019. Physical and mechanical properties of a reversible adhesive for automotive applications. Int. J. Adhes. Adhes. 89, 117–128.

Jambor, A., Beyer, M., 1997. New cars-new materials. Mater. Des. 18, 203–209.

Li, Y., Lin, Z., Jiang, A., 2004. Experimental study of glass-fiber mat thermoplastic material impact properties and lightweight automobile body analysis. Mater. Des. 25, 579–585.

da Silva, L.F.M., Ochsner, A., Adams, R.D., 2011. Handbook of Adhesion Technology, 1st Edition Springer-Verlag, Berlin Heidelberg.

Belingardi, G., Chiandussi, G., 2004. Stress flow in thin walled box beams obtained by adhesive bonding joining technology. Int. J. Adhes. Adhes. 24, 423–439.

Kim, Y.G., Lee, S.J., Lee, D.G., Jeong, K.S., 1997. Strength analysis of adhesively-bonded tubular single lap steel-steel joints under axial loads considering residual thermal stresses. J. Adhes. 60, 125–140.

Raftery, G.M., Harte, A.M., Rodd, P.D., 2009. Bonding of FRP materials to wood using thin epoxy gluelines. Int. J. Adhes. Adhes. 29, 580–588.

Morano, C., Musiari, F., Spennacchio, G.D., Di Lonardo, D., 2019. Experimental analysis of steel joints bonded with automotive grade hot setting structural adhesives. P. I. Mech. Eng. L-J Mat. 233, 2084–2093.

Machado, J.J.M., Marques, E.A.S., da Silva, L.F.M, 2017. Adhesives and adhesive joints under impact loadings: an overview. J. Adhes. 94, 421–452.

Pirondi, A., Nicoletto, G., 2004. Mixed mode I/II fatigue crack growth in adhesive joints. Eng. Fract. Mech. 73, 2557–2568.

ASTM D3433-99. Standard test method for fracture strength in cleavage of adhesives in bonded metal joints (2012).

ISO 25217:2009. Adhesives — determination of the mode I adhesive fracture energy of structural adhesive joints using double cantilever beam and tapered double cantilever beam specimens (2009).

BS 7991:2001. Determination of the mode I adhesive fracture energy, GIC, of structural adhesives using the double cantilever beam (DCB) and tapered double cantilever beam (TDCB) specimens (2001).

Stamoulis, G., Carrere, N., Cognard, J.Y., Davies, P., Badulescu, C., 2016. Investigating the fracture behavior of adhesively bonded metallic joints using the Arcan fixture. Int. J. Adhes. Adhes. 66, 147–159.

ASTM D6671/D6671M-19. Standard test method for mixed mode I-Mode II interlaminar fracture toughness of unidirectional fiber reinforced polymer matrix composites (2013).

ASTM D7905/7905M. Standard test method for determination of the mode ii interlaminar fracture toughness of unidirectional fiber-reinforced polymer matrix composites (2014).

ISO/DIS 15114:2014. Fibre-reinforced plastic composites — determination of the mode II fracture resistance for unidirectionally reinforced materials using the calibrated end-loaded split (C-ELS) test and an effective crack length approach (2014).

Argoud, N., Rousseau, J., Piezel, B., Chettah, A., Cadu, T., Fiore, A., Fontaine, S., 2018. Multi-axial testing of thick adhesive bonded joints of fibre reinforced thermoplastic polymers. Int. J. Adhes. Adhes. 84, 37–47.

Arcan, L., Arcan, M., Daniel, I., 1987. SEM fractography of pure and mixed mode interlaminar fracture in graphite/epoxy composites. ASTM Tech. Publ. 948, 41–67.

Legendre, J., Creachcadec, R., Gilbert, F., Jacquet, D., 2018. A new method to measure the adhesion capability of the metallic surface under shear loading using a modified Arcan test. J. Adhes. 94, 1017–1035.

Yang, X., Xia, Y., Zhou, Q., 2010. A simplified Fe model for pull-out failure of spot welds. Eng. Fract. Mech. 77, 1224–1239.

Hörhold, R., Müller, M., Merklein, M., Meschut, G., 2016. Mechanical properties of an innovative shear-clinching technology for ultra-high-strength steel and aluminium in lightweight car body structures. Weld. World. 60, 613–620.

Patil, S., Lankarani, H., 2019. Characterisation and modelling the strength of EHSS steel grade spot weld for automotive joints and its application for frontal impact load-case. Int. J. Crashworthiness 24, 13–23.

García, S.J., Rodríguez, M.T., Izquierdo, R., Suay, J., 2007. Evaluation of cure temperature effects in cataphoretic automotive primers by electrochemical techniques. Prog. Org. Coat. 60, 303–311.

Ooi, S.K., Cook, W.D., Simon, G.P., Such, C.H., 2000. DSC studies of the curing mechanisms and kinetics of DGEBA using imidazole curing agents. Iranian Polym. J. 41, 3639–3649.

Ciardiello, R., Drzal, L.T., Belingardi, G., 2017. Effects of carbon black and graphene nano–platelet fillers on the mechanical properties of syntactic foam. Compos. Struct. 178, 9–19.